

See discussions, stats, and author profiles for this publication at: <https://www.researchgate.net/publication/221573689>

Blurred Image Region Detection and Classification

Conference Paper · November 2011

DOI: 10.1145/2072298.2072024 · Source: DBLP

CITATIONS

137

READS

3,578

3 authors:



Bolan Su

Institute for Infocomm Research

31 PUBLICATIONS 1,425 CITATIONS

SEE PROFILE



Shijian Lu

Nanyang Technological University

216 PUBLICATIONS 5,213 CITATIONS

SEE PROFILE



Chew Lim Tan

National University of Singapore

427 PUBLICATIONS 11,638 CITATIONS

SEE PROFILE

Some of the authors of this publication are also working on these related projects:



iterative mid point [View project](#)



Image Synthesis [View project](#)

Blurred Image Region Detection and Classification *

Bolan Su^{*+}
subolan@comp.nus.edu.sg

Shijian Lu⁺
slu@i2r.a-star.edu.sg

Chew Lim Tan^{*}
tancl@comp.nus.edu.sg

^{*}School of Computing, National University of Singapore
Computing 1(COM1), 13 Computing Drive, Singapore 117417

⁺Institute for Infocomm Research, Singapore
1 Fusionopolis Way #21-01 Connexis, Singapore 138632

ABSTRACT

Many digital images contain blurred regions which are caused by motion or defocus. Automatic detection and classification of blurred image regions are very important for different multimedia analyzing tasks. This paper presents a simple and effective automatic image blurred region detection and classification technique. In the proposed technique, blurred image regions are first detected by examining singular value information for each image pixels. The blur types (i.e. motion blur or defocus blur) are then determined based on certain alpha channel constraint that requires neither image deblurring nor blur kernel estimation. Extensive experiments have been conducted over a dataset that consists of 200 blurred image regions and 200 image regions with no blur that are extracted from 100 digital images. Experimental results show that the proposed technique detects and classifies the two types of image blurs accurately. The proposed technique can be used in many different multimedia analysis applications such as image segmentation, depth estimation and information retrieval.

Categories and Subject Descriptors

I.4.6 [IMAGE PROCESSING AND COMPUTER VISION]: Segmentation—*Pixel classification*; I.5.4 [PATTERN RECOGNITION]: Application—*Computer Vision*

General Terms

Algorithms

Keywords

Image Blur, Blurred Region Detection and Classification, Singular Value Decomposition, α Channel Map

1. INTRODUCTION

There exists blur in many digital images due to defocus or motion, which is illustrated in Figure 1(a) and (c). Sometimes blur

* Area chair: Bernard Merialdo

Permission to make digital or hard copies of all or part of this work for personal or classroom use is granted without fee provided that copies are not made or distributed for profit or commercial advantage and that copies bear this notice and the full citation on the first page. To copy otherwise, to republish, to post on servers or to redistribute to lists, requires prior specific permission and/or a fee.

MM'11, November 28–December 1, 2011, Scottsdale, Arizona, USA.
Copyright 2011 ACM 978-1-4503-0616-4/11/11 ...\$10.00.

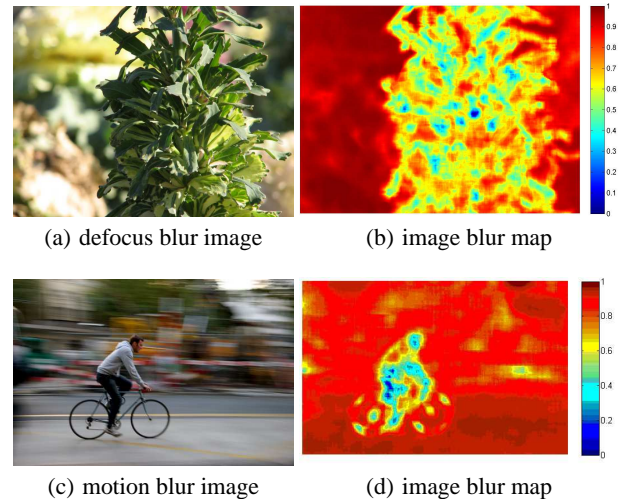


Figure 1: Illustration of the blur map constructed by a singular value feature: (a,c) show a pair of example images that suffer from defocus blur and motion blur; (b,d) show the corresponding blur maps that are constructed based on the proposed singular value feature.

may be produced by the photographer to strengthen photo's expressiveness, but unintentional blur will decrease the image quality, which is caused by incorrect focus, object motion, hand shaking and so on. In any cases, automatic image blurred region detection and classification are useful for learning the image information, which can be used in different multimedia analysis applications such as image segmentation, depth recovery and image retrieval.

Many blur detection techniques are based on edge sharpness information [7, 9]. However, these edge sharpness based methods cannot distinguish either the blurred/non-blurred image regions or the type of image blurs. And Kovacs and Sziranyi's method [3] extract the unblur region using blind deconvolution. Based on the observation that blurred images usually lack high frequency information, some techniques [8, 6] detect image blurs using low pass filtering, without applying the deconvolution.

In this paper, we propose an automatic image blurred detection and classification technique that first detects blurred regions within a single image and then identifies the blur type of the blurred image regions. The contributions of our work can be summarized in several aspects.

- First, we observe the connection between image blurs and

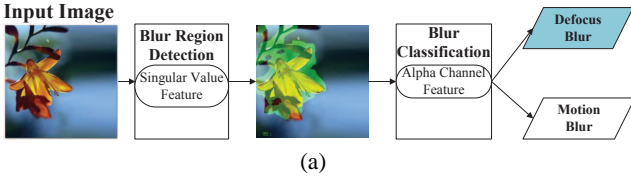


Figure 2: Framework of the proposed image blurred region detection and classification technique.

singular value distributions and accordingly design a blur metric that detects blurred regions from a single image accurately.

- Second, we capture the distribution pattern of the gradient of the alpha channel to differentiate motion and defocus blur effectively.
- Third, we build an automatic blur detection and classification system that requires neither image deblurring nor blur kernel estimation. The built system can also be used in many other applications such as image segmentation, image enhancement and image retrieval.

2. THE PROPOSED SYSTEM

The proposed technique first constructs a blur map that encodes the blur degree of an image. The blur degree is estimated by the ratio between the first few most significant singular values and all singular values that are computed over a local image patch surrounding each image pixel. Such estimation is based on the observation that the first few most significant eigen-images of a blurred image patch usually have higher weights (i.e. singular values) than an image patch with no blur (because image blurs often suppress the high-frequency image details that is reflected within those less significant eigen-images). Once the blurred image regions are extracted, the blur types of those blurred regions are further identified based on the gradient distribution patterns of the alpha channels.

The overall framework is illustrated in Figure 2. The non blurred region is first extracted from the input image, which is marked by green color, and then the blurred region is classified into defocus blur as highlighted in the blue box.

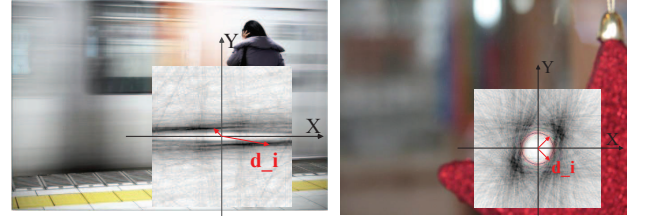
3. IMAGE BLUR FEATURES

This section describes the two image features that are used in our proposed blur detection and classification technique. One feature is a singular value feature that can be used as a blur metric to detect image blur effectively and accurately. The other feature is an alpha channel feature that can be used for blur type classification.

3.1 Singular Value Feature

Singular value decomposition (SVD) is one of the most useful techniques in linear algebra, and has been applied to different areas of computer science. Given an image I , its SVD can be represented by $I = U\Lambda V^T$ where U, V are orthogonal matrices and Λ is a diagonal matrix that is composed of multiple singular values arranged in decreasing order. The image can therefore be decomposed into multiple rank 1 matrices (which are also called eigen-images) [1] as follows:

$$I = \sum_{i=1}^n \lambda_i \mathbf{u}_i \mathbf{v}_i^T \quad (1)$$



(a) motion blur image

(b) defocus blur image

Figure 3: a pair of example images suffering from motion blur image and defocus blur and their corresponding $\nabla\alpha$ distributions in Hough space (a clear white circle region appears in $\nabla\alpha$ distribution of the defocus blur image as highlighted by a red color circle in (b)).

where the $\mathbf{u}_i, \mathbf{v}_i$, and λ_i are the column vectors of U, V and diagonal terms of Λ . Under the framework of digital image compression, the image I can be approximated by I_k that sums up the first k components.

As Equation 1 shows, the singular value decomposition actually decomposes an image into a weighted summation of a number of eigen-images where the weights are exactly the singular values themselves. Therefore, the compressed image which omits the small singular value in tail actually replaces the original image by a coarse approximation. Those eigen-images with a small singular value which often capture detailed information are instead discarded.

Such situation is similar to the image blurring that keeps shape structures at large scales but discards image details at small scales. From another viewpoint, those eigen-images in Equation 1 provide different scale-space analysis of the image [1], i.e., the first few most significant eigen-images work on large scales that provide rough shapes of the image while those latter less significant eigen-images encode the image details. Suppose that an image I is convoluted with a Point Spread Function (PSF) H as follows:

$$I * H = \sum_{i=1}^n \lambda_i (\mathbf{u}_i \mathbf{v}_i^T) * H \quad (2)$$

where the convolution operator $(\mathbf{u}_i \mathbf{v}_i^T) * H$ tends to increase the scale-space of eigen-images and accordingly causes a loss of high-frequency details. In other word, those small singular values that match to small scale space eigen-images correspond to larger scale-space eigen-images after convolution. As a result, the image details are weakened and those large scale-space eigen-images get higher weights. For a blurred image, the first few most significant eigen-images therefore usually have much higher weights (i.e. singular values) compared with that of a clear image. We thus propose a singular value feature that measures the blurry degree of an image as follows:

$$\beta_1 = \frac{\sum_{i=1}^k \lambda_i}{\sum_{i=1}^n \lambda_i} \quad (3)$$

where λ_i denotes the singular value that is evaluated within a local image patch for each image pixel. As Equation 3 shows, the singular feature is actually the ratio between the first k most significant singular value and all singular values.

Generally, blurred image regions have a higher blur degree compared with clear image regions with no blurs, which is shown in



Figure 4: Selected samples of blurred/non-blurred image regions from our dataset.

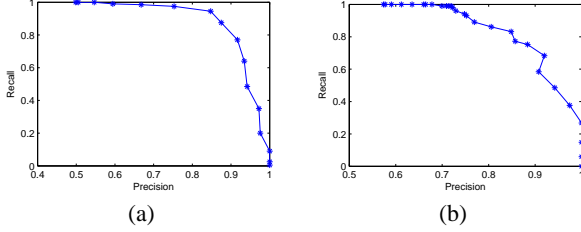


Figure 5: Illustration of the Recall-Precision curve of our classification method. (a) the recall-precision curve of 'blur' in blur/nonblur classification using singular value feature. (b) the recall-precision curve of 'defocus blur' in motion/defocus blur classification using alpha channel feature.

Figure 1(b) and (d). So an image pixel will be classified into blurred region if its β_1 is larger than a threshold, otherwise, it will be categorized as non blurred region.

3.2 Alpha Channel Feature

Once the image blur is detected, the image blur type needs to be identified as either motion blur or defocus blur. We use the two-layer image composition model [5], in which an image I is viewed as a combination of an image foreground F and an image background B as follows:

$$I = \alpha F + (1 - \alpha)B \quad (4)$$

where α lies between 0 and 1. In a clear image, most of the values of α are either 1 or 0. But in a blurred image, the foreground and background tend to mix together, most of the value of α lie at the boundary between foreground and background become pure decimal.

An alpha channel model constraint [2] has been reported for motion blur images, which is defined as $\nabla\alpha \cdot \mathbf{b} = \pm 1$. \mathbf{b} is a 2×1 vector, denotes the blur extension in horizontal and vertical direction. The blur kernels \mathbf{b} of motion blurred images are usually directional, so the distribution of $\nabla\alpha$ will be lines, which is shown in Figure 3(a). But the image pixel intensities will spread out with constant steps at every directions after blurred for defocus blurred images, so the elements of $\nabla\alpha$ will have similar magnitude values but different angles. And then the $\nabla\alpha$ distribution will look like a circle, as shown in Figure 3(b).

So we evaluate the circularity of shape pattern of $\nabla\alpha$ distribution. We calculate the distances from the center to nearest salient points(dark spot) at different directions on the $\nabla\alpha$ distribution to obtain an array d_1, d_2, \dots, d_n , where d_i denotes the estimated distance at one direction, which is shown in Figure 3. We define the alpha channel feature β_2 as the variation of the distance array, which is shown in Equation 5.



Figure 6: Illustration of blurred and non-blurred image region extractions by several example images: the red curves separate the blurred and non-blurred images regions where the image in (a) has a blurred background and the image in (b) has a blurred foreground.

$$\beta_2 = Var\{d_1, d_2, \dots, d_n\} \quad (5)$$

The motion blurred image regions will have much larger β_2 values compared with defocus blurred image regions. So a threshold is used on β_2 to classify the type of blurred regions into either motion or defocus.

4. EXPERIMENTS AND DISCUSSIONS

4.1 Blur Region and Type Classification

Our blur detection and classification features are tested on different images. Those images are first cropped into smaller regions so that they contain only blur or clear region. We generate 200 clear image regions, 100 defocus blur image regions, and 100 motion blur image regions in total from 100 digital images. Some examples of our dataset are shown in Figure 4.

Figure 5 shows the recall-precision curve of our method. The threshold for singular value feature varies from 0 to 1, with a step 0.05, while the threshold of alpha channel feature changes in a range [0,0.4], the interval is 0.01. And the method produce best accuracy for blur/nonblur classification when singular value threshold is 0.75, the accuracy is 88.78%. The best accuracy for motion/defocus classification is 80% when the alpha channel threshold is 0.12. Compared with Liu et.al.'s method [6], which reports maximum 76.98% accuracy for blur/nonblur classification and 78.84% for motion/defocus blur classification, our method is simpler yet performs great.

4.2 Blur Region Segmentation

We then use our technique to extract blurred regions of images. A blurred region is extracted based on the constructed singular value blur map. And a blur mask is built based on the threshold obtained in the previous subsection to divide blurred/non blurred regions. To evaluate the accuracy, we first manually extracted the blurred regions of 10 partially blurred images as ground truth. The blurred image regions extracted by our proposed method is then evaluated based on their comparison with the ground truth image regions. The accuracy measurement of our region extraction is defined as the ratio of the correctly segmented pixels and the total image pixels. Our experiments show that the blurred region extraction accuracy (by our proposed method) is 83% on averaged over the 10 images. Our method can successfully extracts the blurred image regions, as shown in Figure 6.

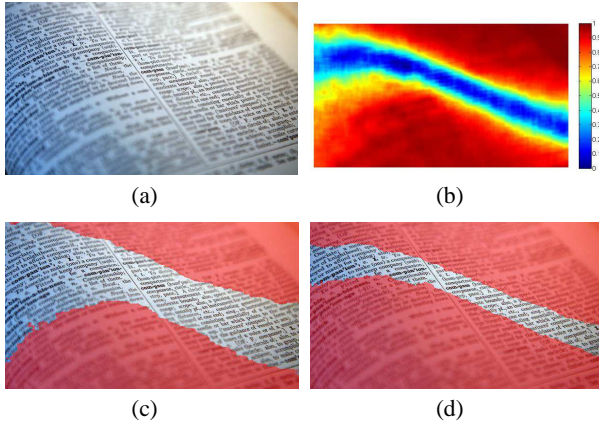


Figure 7: The document image in (a) contains defocus blur of different extents. Its corresponding singular value map is shown in (b), those regions with different blur degrees are highlighted in different color. (c) and (d) show the two extracted blurred image regions of (a) when the threshold is set at 0.91 and 0.76, respectively.

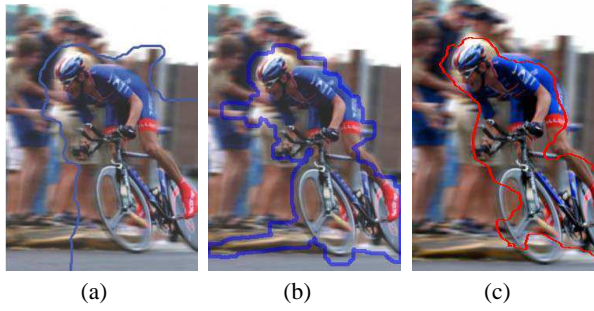


Figure 8: Comparison of blurred image region extraction: (a-c) show the blurred image regions that are extracted by using Levin's method [5], Liu et al.'s method [6], and our proposed method, respectively.

On the other hand, the size of extracted blurred image regions depends on the singular value threshold because there is no clear boundary between blurred and non-blurred image regions. Figure 7(a) shows a blurred document image example and Figure 7(b) shows the singular value blur map of the example image that illustrates blur degree variation. Different blurred image extraction results can be obtained when different thresholds are set. As shown in Figure 7, two different blurred image regions in (c) and (d) can be extracted from (a) based on the thresholds of 0.91 and 0.76, respectively. We also compare our proposed technique with Liu et al. [6] and Levin's [4] based on a public image shown in Figure 8, which also produces good segmentation result.

4.3 Blur Degree Estimation

Lastly, we can use our blur detection features to rank the blur level of images. The blur degree of an image is affected by two aspects: one is the blur extent of the whole image, which can be evaluated by the singular value feature β_1 ; the other is the ratio of the size of blur area to the whole image size. The blur degree of an image is then given as follows:

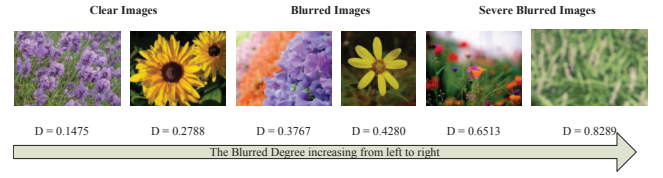


Figure 9: Images ranked based on the estimated blurry degree D : the proposed D in Equation 6 captures the image blurry degree properly, i.e., images are blurred more severely with the increase of D .

$$D = k\beta_1 + (1 - k)\left(\frac{\Omega_b}{\Omega}\right) \quad (6)$$

where k is a weight that is set to 0.5 to give equal weights to the two aspects, Ω_b denotes the size of blurred image regions, Ω denotes the whole image size. Those severely blurred images should have large values on β_1 and $\frac{\Omega_b}{\Omega}$, and then the degree D . Figure 9 shows an array of example images that are ranked by the blur degree estimated by our proposed technique, which are sorted properly.

5. CONCLUSION

In this paper, we propose an image blurred region detection and classification method that can automatically detect blurred image regions and classifies the blur types without either image deblurring or kernel estimation. We construct a new blur metric: singular value feature, and use it to detect the blurred regions of an image. We also analyze the alpha channel information and classify the blur type of the blurred image regions into defocus blur or motion blur, respectively. Our proposed method is simple and effective. Experiments show that our method works for different kinds of images and can also be used for different multimedia analysis applications such as depth recovery, information retrieval and segmentation.

6. REFERENCES

- [1] H. Andrews and C. Patterson. Singular value decompositions and digital image processing. *IEEE Transaction on Acoustics, Speech and Signal Processing*, 24:26–53, 1976.
- [2] S. Dai and Y. Wu. Motion from blur. *CVPR*, 2008.
- [3] L. Kovács and T. Szirányi. Focus area extraction by blind deconvolution for defining regions of interest. *IEEE Transaction on Pattern Analysis and Machine Intelligence*, 29:1080–1085, 2007.
- [4] A. Levin. Blind motion deblurring using image statistics. *Advances in Neural Information Processing Systems*, 2007.
- [5] A. Levin, A. Rav-Acha, and D. Lischinski. Spectral matting. *IEEE Transactions on Pattern Analysis and Machine Intelligence*, 30:1699–1712, 2008.
- [6] R. Liu, Z. Li, and J. Jia. Image partial blur detection and classification. *CVPR*, 2008.
- [7] P. Marziliano, F. Dufaux, S. Winkler, and T. Ebrahimi. A non-reference perceptual blur metric. *ICIP*, 3:57–60, 2002.
- [8] J. D. Rugna and H. Konik. Automatic blur detection for metadata extraction in content-based retrieval context. *SPIE*, 5304:285–294, 2003.
- [9] H. Tong, M. Li, H. Zhang, and C. Zhang. Blur detection for digital images using wavelet transform. In *Proceedings of IEEE International Conference on Multimedia&Expo*, pages 17–20, 2004.